Shootin1: a protein involved in the organization of an asymmetric signal for neuronal polarization

Michinori Toriyama,[1] Tadayuki Shimada,[1] Ki Bum Kim,[1] Mari Mitsuba,[1] Eiko Nomura,[1] Kazuhiro Katsuta,[1] Yuichi Sakumura,[2] Peter Roepstorff,[3] and Naoyuki Inagaki[1]

[1]Division of Signal Transduction and [2]Bioinformatics Unit, Nara Institute of Science and Technology, Ikoma 630-0192, Japan
[3]Department of Biochemistry and Molecular Biology, University of Southern Denmark, DK-5230 Odense M, Denmark

Neurons have the remarkable ability to polarize even in symmetrical in vitro environments. Although recent studies have shown that asymmetric intracellular signals can induce neuronal polarization, it remains unclear how these polarized signals are organized without asymmetric cues. We describe a novel protein, named shootin1, that became up-regulated during polarization of hippocampal neurons and began fluctuating accumulation among multiple neurites. Eventually, shootin1 accumulated asymmetrically in a single neurite, which led to axon induction for polarization. Disturbing the asymmetric organization of shootin1 by excess shootin1 disrupted polarization, whereas repressing shootin1 expression inhibited polarization. Overexpression and RNA interference data suggest that shootin1 is required for spatially localized phosphoinositide-3-kinase activity. Shootin1 was transported anterogradely to the growth cones and diffused back to the soma; inhibiting this transport prevented its asymmetric accumulation in neurons. We propose that shootin1 is involved in the generation of internal asymmetric signals required for neuronal polarization.

Introduction

The basic function of neurons is to receive, integrate, and transmit signals. To do so, most neurons develop polarity by forming a single axon and multiple dendrites (Craig and Banker, 1994; Winckler and Mellman, 1999; Da Silva and Dotti, 2002; Horton and Ehlers, 2003). Neurons have the remarkable ability to polarize even in symmetrical in vitro environments (Dotti et al., 1988; Craig and Banker, 1994). The processes of their polarization have been extensively studied using hippocampal neurons. These cells first form several immature neurites that are capable of becoming either axons or dendrites. One of the neurites then acquires axonal characteristics, whereas the others later become dendrites. Hippocampal neurons must use a robust internal mechanism that guarantees polarization, as they generate a single axon and multiple dendrites even when polarity is altered by axonal amputation (Dotti and Banker, 1987; Goslin and Banker, 1989).

Recent studies have begun to define the signaling pathways involved in neuronal polarization. Esch et al. (1999) reported that the extracellular signals laminin and neuron-glia cell adhesion molecule can specify which neurite will become an axon. As effectors of spatial signals, rearrangements of the cytoskeleton are important, as actin filament instability (Bradke and Dotti, 1999) and tubulin assembly by collapsin response mediator protein-2 (Inagaki et al., 2001; Arimura and Kaibuchi, 2005) are reported to initiate axon formation. Recent work has shown that spatially localized intracellular signaling pathways, including phosphoinositide-3-kinase (PI 3-kinase), phosphatidylinositol (3,4,5) triphosphate, the mPar3–mPar6–aPKC complex (with the exception of some neurons in *Drosophila melanogaster*; Rolls and Doe, 2004), Cdc42, Rap1B, STEF/Tiam1, Rac, Akt, adenomatous polyposis coli, and glycogen synthase kinase-3β, are involved in axon specification for neuronal polarity formation (Shi et al., 2003, 2004; Menager et al., 2004; Schwamborn and Puschel, 2004; Jiang et al., 2005; Nishimura et al., 2005; Yoshimura et al., 2005), and PI 3-kinase is implicated as an upstream molecule in these events (Shi et al., 2003; Arimura and Kaibuchi, 2005; Wiggin et al., 2005).

In spite of this progress, the mechanism and logic of how the polarized distribution of intracellular signals originates in the absence of external asymmetric cues remain elusive.

M. Toriyama and T. Shimada contributed equally to this paper.

Correspondence to Naoyuki Inagaki: ninagaki@bs.naist.jp

K.B. Kim's present address is Laboratory of Cell Signal Transduction, School of Life Science and Biotechnology, Korea University, Seoul, 136-701 Korea.

Abbreviations used in this paper: 2DE, 2D electrophoresis; CMFDA, 5-chloromethylfluorescein diacetate; DIV, day in vitro; E, embryonic day; miRNA, microRNA; mRFP, monomeric red fluorescent protein; P, postnatal day; PI 3-kinase, phosphoinositide-3-kinase.

The online version of this article contains supplemental material.

The Journal of Cell Biology, Vol. 175, No. 1, October 9, 2006 147–157
http://www.jcb.org/cgi/doi/10.1083/jcb.200604160

During the polarization of cultured hippocampal neurons, undifferentiated neurites undergo competitive elongation with each other. When one of them exceeds the others by a critical length, it rapidly elongates to become an axon (Goslin and Banker, 1989). This observation led to the proposal that a positive feedback loop and negative regulation among neurites are necessary for neuronal polarization (Goslin and Banker, 1989; Andersen and Bi, 2000; Banker, 2003). A locally acting positive feedback loop may amplify a small stochastic increase in signals until it exceeds a threshold to induce an axon, and negative regulation may also be important to prevent the formation of surplus axons. However, little is known about the molecular basis of such regulation.

To approach this problem, we performed proteome analyses of cultured hippocampal neurons using highly sensitive large-gel 2D electrophoresis (2DE), which can detect ∼11,000 protein spots over a dynamic range of $1–10^5$ (Inagaki and Katsuta, 2004). We describe a novel brain-specific protein, named shootin1. Our data suggest that shootin1 organizes its own polarized distribution to break neuronal symmetry through the PI 3-kinase pathway.

Results

Identification of shootin1 by double proteome screenings

Cultured hippocampal neurons are a well-established system to study spontaneous neuronal polarization (Dotti et al., 1988; Craig and Banker, 1994). They extend several minor processes during the first 12–24 h after plating (stages 1–2). One of these processes then begins to elongate continuously to become an axon (stage 3). The transition from stage 2 to 3 is the initial step of polarization (Fig. 1 A).

To identify proteins involved in neuronal polarization, we performed two separate proteome analyses of cultured rat hippocampal neurons using a 93- × 103-cm large-gel 2DE (Inagaki and Katsuta, 2004). One was to detect proteins up-regulated during neuronal polarization (Fig. 1 A): we screened ∼6,200 protein spots on 2DE gels and detected 277 that were consistently up-regulated during the transition from stage 2 to 3 ($n \geq 3$). The second analysis screened proteins enriched in axons (Fig. 1 B). Hippocampi dissected from embryonic day (E) 18 rat embryos were cut into ∼1-mm blocks and cultured on plastic dishes, where they formed complicated networks of radial axons in 2 wk. The explants' somatodendritic parts were then separated from the axon networks, and both were compared by 2DE. By screening ∼5,200 protein spots, we detected 200 spots enriched in the axon samples ($n \geq 3$).

A total of 23 spots were detected by both screenings. Tryptic digestion and mass spectrometry of one of them, located at a molecular mass of 60 kD and pI = 5.3 in gels (Fig. 1, A and B), identified 10 peptides whose sequences corresponded to the human cDNA sequence KIAA1598 encoding a 5′-truncated ORF of 446 amino acids. A BLAST search identified four human EST clones (BI598285, BG720033, BE568283, and BI457767) and suggested that 10 additional amino acids are present in the complete ORF. We then cloned the cDNAs for the rat and human ORFs and termed them *shootin1*.

Rat and human *shootin1* encode proteins of 456 amino acids and predicted molecular masses of 52.4 and 52.6 kD, respectively (Fig. 1 C). Domain searching revealed that shootin1 contains three coiled-coil domains and a single proline-rich region (Fig. 1 D). It does not show significant homology to previously known polypeptides, however, suggesting that it belongs to a novel class of proteins. Database searches also identified a mouse orthologue of *shootin1* (Fig. 1 C) and partial ORFs in *Macaca fascicularis*, chick, zebrafish, and *Fugu rubripes*. Invertebrate homologues of *shootin1* were not found in the databases. Thus, shootin1 is probably a late addition to the genome during the evolution of animals.

Shootin1 is brain specific and highly up-regulated during polarization

We raised an antibody against recombinant shootin1. It recognized a 60-kD band, corresponding to the apparent M_r of native and recombinant shootin1, in immunoblots of rat cultured hippocampal neurons (Fig. 1 E, arrowhead). Consistent with the 2DE data for the metabolically labeled protein (Fig. 1 A), the level of shootin1 expression increased remarkably during stage 2/3 transition (14.4-fold increase; $n = 4$; $P < 0.005$) and remained high until day in vitro (DIV) 14, thereafter returning to a low level by DIV28 when expression of the presynaptic protein synaptophysin increased (Fig. 1 E). Immunoblot analysis of various rat tissues detected shootin1 in postnatal day (P) 4 and adult brains but not in other tissues, suggesting that shootin1 is a brain-specific protein (Fig. 1 F). Expression of shootin1 was relatively low on E15, peaked around P4, and decreased to a low level in the adult brain (Fig. 1 G). Thus, the expression of shootin1 is up-regulated, both in hippocampal neurons and in brain, during the period of axon formation and elongation.

Shootin1 accumulates in axonal growth cones during the stage 2/3 transition

Next, we examined the localization of shootin1 in cultured hippocampal neurons. Immunocytochemical analysis showed a faint and diffuse staining of endogenous shootin1 in early stage 2 neurons (18–24 h in culture; unpublished data). In late stage 2, moderate amounts of shootin1 appeared in some growth cones of minor processes (Fig. 1 H). We used a volume marker, 5-chloromethylfluorescein diacetate (CMFDA), to measure the relative concentration of shootin1: it was calculated by using CMFDA as an internal standard (shootin1 immunoreactivity/CMFDA staining). The relative concentration of shootin1 accumulated in the growth cones of late stage 2 neurons was 2–4 times higher than that in the cell body (Fig. 1 H, arrowheads). In stage 3, shootin1 accumulated strongly in axonal growth cones (Fig. 1 I, arrows): 100% of axonal growth cones showed accumulation ($n = 19$). The relative concentration of shootin1 in the axonal growth cones of stage 3 neurons was ∼10 times higher than that in the other regions. Notably, the accumulation seen at late stage 2 in minor processes mostly disappeared in stage 3 (Fig. 1 I, arrowheads), with only 12% of the processes showing accumulation ($n = 68$). Shootin1 concentration in the cell body remained low throughout stages 2 and 3 (Fig. 1, H and I, asterisks).

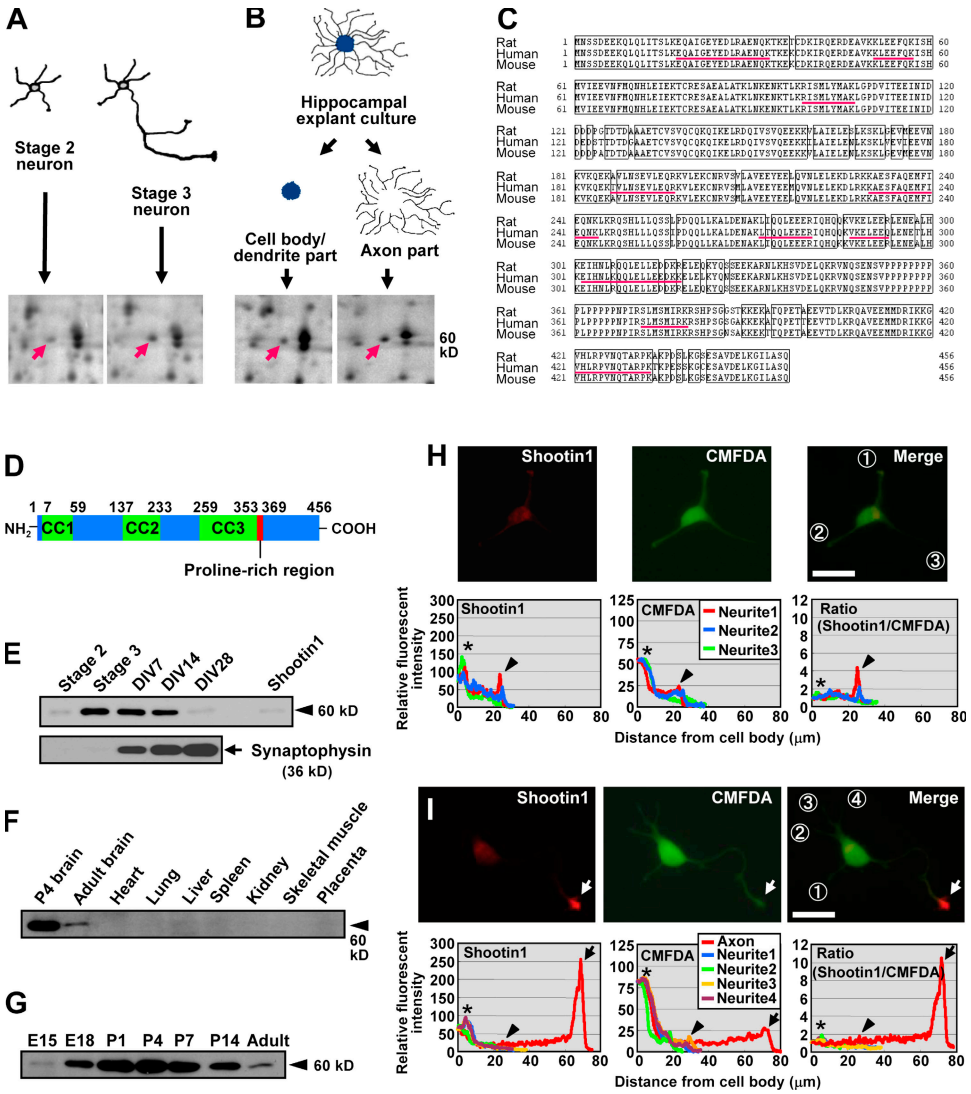

Figure 1. **Identification, structure, expression, and intracellular localization of shootin1.** (A) Differential 2DE analysis of proteins in stage 2 (cultured for 14 h) and stage 3 (cultured for 62 h) hippocampal neurons. The arrows indicate the protein spot of shootin1 enriched in the stage 3 sample (stage 3/2 = 3.2; n = 12; $P < 0.001$). (B) Differential 2DE analysis of proteins in cell body/dendrite and axon samples. The arrows indicate the same protein spot shown in A, which is also enriched in the axon samples (axon/somatodendrite = 1.6; n = 7; $P < 0.005$). (C) Amino acid sequence of rat, human, and mouse shootin1. Sequences of the peptides identified by mass spectrometry analysis are underlined. (D) Schematic representation of rat shootin1, showing three coiled-coil domains (CC1–3) and a single proline-rich region. (E) Immunoblot analysis of purified recombinant shootin1 and shootin1 in cultured rat hippocampal neurons at different stages. Immunoblot data of synaptophysin are also shown. (F) Immunoblot analysis of shootin1 in adult rat tissues and P4 brain. (G) Immunoblot analysis of shootin1 in rat brains at various developmental stages. (H and I) Immunofluorescent localization of shootin1 in late stage 2 (H) and stage 3 (I) hippocampal neurons. Neurons were double stained with anti-shootin1 antibody (red) and a volume marker CMFDA (green). Quantitative profiles show the relative fluorescence intensities of shootin1 and CMFDA and relative concentration of shootin1 (shootin1 immunoreactivity/ CMFDA staining). Arrows, arrowheads, and asterisks denote axonal growth cones, minor process growth cones, and cell bodies, respectively. Bars, 20 μm.

The accumulation of shootin1 in axonal growth cones was observed until stage 5 (unpublished data).

In stage 2, shootin1 shows fluctuating accumulation in multiple growth cones, concurrent with neurite elongation

To analyze the localization of shootin1 in living neurons, we monitored fluorescent images of EGFP-shootin1 expressed in hippocampal neurons under the cytomegalovirus promoter every 5 min. Although relatively high levels of EGFP-shootin1 appeared in the soma, indicating that the expression exceeds the endogenous levels, its distribution in neurites was virtually identical to that of endogenous shootin1 (see the following paragraph). Consistent with the immunocytochemical data, we observed accumulation of EGFP-shootin1 in the growth cones of minor processes in late stage 2 neurons (Fig. 2 A). As reported previously (Goslin and Banker, 1989), minor processes showed competitive extension and retraction before polarization. Surprisingly, "hotspots" of EGFP-shootin1 accumulation repeatedly appeared and disappeared in the growth cones of individual neurites (n = 11 cells; Fig. 2 A and Video 1, available at http://www.jcb.org/cgi/content/full/jcb.200604160/DC1). Most of the neurites elongated in conjunction with EGFP-shootin1 accumulation and, conversely, retracted as EGFP-shootin1

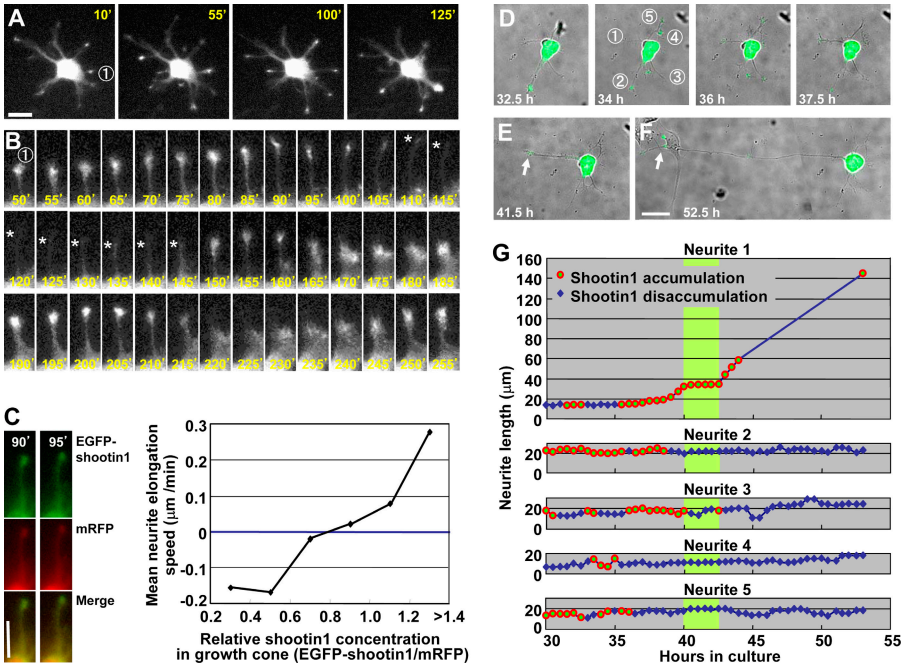

Figure 2. **Dynamic accumulation of EGFP-shootin1 in growth cones of hippocampal neurons.** (A) A stage 2 hippocampal neuron expressing EGFP-shootin1 was observed under a time-lapse fluorescence microscope every 5 min. The full video is presented in Video 1 (available at http://www.jcb.org/cgi/content/full/jcb.200604160/DC1). (B) The pictures represent a series of enlarged images of neurite 1 in A taken every 5 min. Asterisks indicate the front edge of the neurite. (C) Correlation between neurite elongation speed and EGFP-shootin1 levels in growth cones. Stage 2 hippocampal neurons expressing EGFP-shootin1 (green) and mRFP (red) was observed under a time-lapse fluorescence microscope every 5 min. Relative levels of EGFP-shootin1 and mRFP in growth cones were quantified using Multi Gauge ($n = 315$). Relative concentration of EGFP-shootin1 in growth cones was calculated by using mRFP as an internal standard (EGFP-shootin1/mRFP), and the neurite elongation speeds during the next 5 min were measured. (D–F) A hippocampal neuron expressing EGFP-shootin1 was observed by time-lapse fluorescence microscopy every 30 min. The full video is presented in Video 2. Arrows indicate EGFP-shootin1 accumulation in the growth cone of the nascent axon. (G) Elongation of neurites 1–5 shown in D. The circles denote growth cones with apparent shootin1 accumulation, and the diamonds indicate growth cones without the accumulation. The green shade denotes the period when the nascent axon (neurite 1) showed exclusive and continuous accumulation before rapid elongation. Bars, 20 μm.

disappeared (Fig. 2 B). To measure relative concentration of EGFP-shootin1 in growth cones, we used the volume marker monomeric red fluorescent protein (mRFP): it was calculated by using mRFP as an internal standard (EGFP-shootin1/mRFP). By quantifying EGFP-shootin1 and mRFP in growth cones and neurite elongation speed, we found a clear dose dependency of neurite elongation rate on shootin1 concentration in the growth cones of stage 2 neurons (Fig. 2 C).

Shootin1 accumulates asymmetrically in a single neurite before polarization

We continued observations until the neurons entered stage 3. Because long exposure to UV light damaged the cells, images were recorded every 30 min ($n = 3$; Fig. 2, D–G; and Video 2, available at http://www.jcb.org/cgi/content/full/jcb.200604160/DC1). After stage 2, when EGFP-shootin1 accumulation fluctuated in individual neurites (Fig. 2 D), the neurons entered a phase in which one of the neurites was 10–15 μm longer than the others (Fig. 2, E and G; and Fig. S1). In most cases, this neurite would later become an axon (Goslin and Banker, 1989, 1990). In the longest neurites, accumulation of EGFP-shootin1 stabilized in the growth cone (Fig. 2 E and Fig. S1, neurite 1, arrows). Simultaneously, the level of EGFP-shootin1 in its sibling neurites decreased dramatically (neurites 2–5). In this period, the mean number of neurites that showed EGFP-shootin1 accumulation decreased to 1.13 ($n = 30$). The longest neurites then underwent rapid elongation and the cells entered stage 3 (Fig. 2, F and G; and Fig. S1). Consistent with the immunocytochemical data (Fig. 1 I), EGFP-shootin1 remained highly concentrated in axonal growth cones during stage 3, whereas it disappeared from the growth cones of minor processes (Fig. 2, F and G; and Fig. S1). The dynamic shift of shootin1 accumulation into the nascent axon raises the possibility that it provides an intracellular asymmetric signal for neuronal polarization.

Excess levels of shootin1 disturb its asymmetric distribution and induce formation of surplus axons

To examine whether the asymmetric accumulation of shootin1 in a single neurite is important for neuronal polarization, we overexpressed EGFP-shootin1 or myc-tagged shootin1 (myc-shootin1) in hippocampal neurons under the stronger β-actin promoter. A high level of EGFP-shootin1 was detected in the soma, with its frequent transport from the soma to growth cones (Fig. 3 A, arrowheads; and Video 3, available at http://www.jcb.org/cgi/content/full/jcb.200604160/DC1). This in turn resulted in more continuous accumulation of EGFP-shootin1 in multiple growth cones (Fig. 3 A, arrows; compared with the dynamic fluctuation of a lower level of EGFP-shootin1 in Fig. 2, A and B, and Video 1) and ectopic accumulation of myc-shootin1 in minor process growth cones in stage 3 neurons (Fig. 3 B, arrowheads). These results suggest that the limited amount of shootin1 is essential for its asymmetric accumulation in a single neurite.

We further cultured the neurons with overexpressed myc-shootin1 until DIV7. Remarkably, 47 ± 2.1% ($n = 3$; 71 neurons examined; $P < 0.0001$, compared with myc-GST) of the neurons bore more than one (two to four) axons that were immunostained by the axon-specific markers anti–tau-1 (Fig. 3 C) and anti-synaptophysin (Fig. S2 A, available at http://www.jcb.org/cgi/content/full/jcb.200604160/DC1) antibodies but were immunonegative for the dendrite-specific marker anti-MAP2

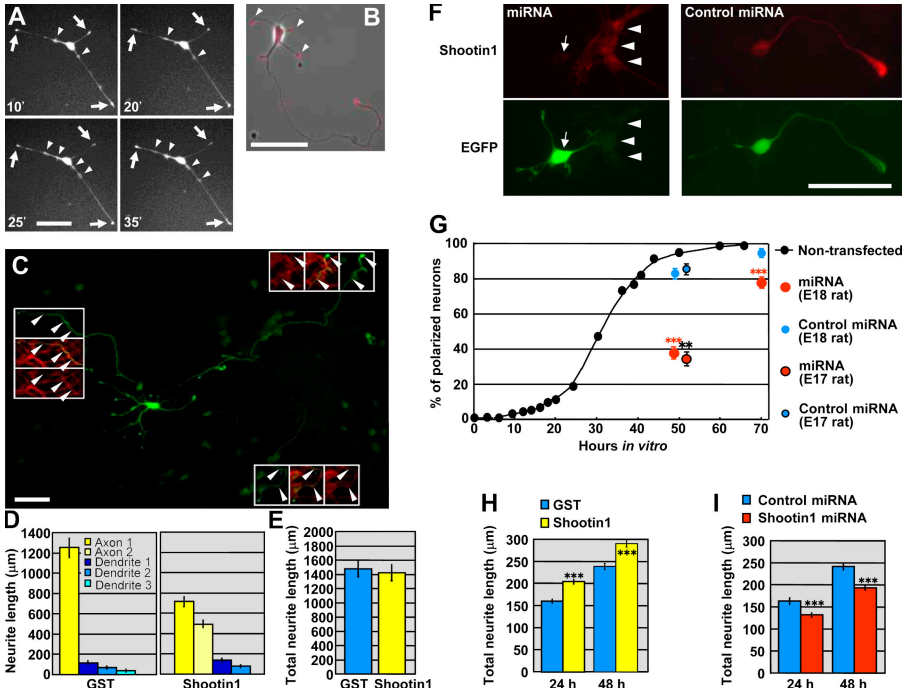

Figure 3. **Effects of shootin1 overexpression and RNAi on polarization of hippocampal neurons.** (A) A neuron overexpressing EGFP-shootin1 was observed every 5 min under a time-lapse fluorescence microscope. The full video is presented in Video 3 (available at http://www.jcb.org/cgi/content/full/jcb.200604160/DC1). Arrows indicate EGFP-shootin1 accumulated at a high level in growth cones. Arrowheads indicate frequent transport of shootin1 from the cell body to the growth cones. (B) Stage 3 neurons overexpressing myc-shootin1 were immunostained by anti-myc antibody (red). Arrowheads indicate myc-shootin1 aberrantly accumulated in the growth cones of minor processes. (C) Hippocampal neurons overexpressing myc-shootin1 were cultured for 7 d and then double immunostained by anti-myc (green) and anti–tau-1 (red) antibodies. Arrowheads indicate axons labeled by anti–tau-1 antibody. (D) Quantification of the neurite lengths of the neurons (DIV7) with surplus axons. The lengths of the longest and secondary axons and dendrites were measured in neurons overexpressing myc-shootin1 ($n = 26$) or myc-GST ($n = 27$). Data present neurite length as means ± SE. (E) Quantification of the total neurite lengths of the neurons (DIV7) overexpressing myc-shootin1 or myc-GST. (F) Neurons transfected with the miRNA or a control miRNA vector were cultured for 50 h. They were then fixed and immunostained with anti-shootin1 antibody. The vectors for miRNA and control miRNA expressions are designed to coexpress EGFP. (G) Neurons prepared from E18 or E17 embryo and transfected with the miRNA or a control miRNA vector were cultured. Data present percentages of neurons bearing axons (stage 3 neurons) as means ± SE (**, $P < 0.02$; ***, $P < 0.002$; $n = 3$; a total of 752 neurons were examined). Black dots present percentages of nontransfected neurons bearing axons. (H and I) Quantification of the total neurite lengths of the neurons overexpressing myc-shootin1 or myc-GST (H) or expressing shootin1 miRNA or control miRNA (I). Data present neurite length as means ± SE (***, $P < 0.0005$; $n = 3$; a total of 761 neurons for H and 568 neurons for I were examined). Bars, 50 μm.

antibody (Fig. S2 B). In contrast, only 2.5 ± 1.4% ($n = 3$; 81 neurons examined) of control neurons with overexpressed myc-GST formed supernumerary axons. On DIV4, 32 ± 1.8% of neurons overexpressing shootin1 bore multiple axons ($n = 3$; 209 neurons examined; $P < 0.002$, compared with GST) that were immunoreactive for tau-1 and anti-synaptophysin antibodies but were immunonegative for anti-MAP2 antibody. On the other hand, 10 ± 2.5% of control neurons overexpressing GST bore multiple axons ($n = 3$; 191 neurons examined). At 50 h in culture, 21 ± 0.9% of neurons overexpressing shootin1 bore multiple axon-like neurites ($n = 3$; 226 neurons examined; $P < 0.001$, compared with GST) that were immunoreactive for tau-1, whereas only 6 ± 1.2% of neurons overexpressing GST bore multiple axon-like neurites ($n = 3$; 173 neurons examined). We also quantified the length of the neurites. Neurites labeled by axonal markers were markedly longer than dendrites (Fig. 3 D). Interestingly, the sum of the length of neurites in neurons overexpressing shootin1 was similar to that in control neurons on DIV7 (Fig. 3 E) and DIV4 (not depicted). Hippocampal neurons elongate axons rapidly (43 μm/d) from stages 3 to 5 (DIV7; Dotti et al., 1988). We consider that the limited amount of structural components produced in cell bodies similarly limits the total neurite elongation in shootin1-overexpressing and control neurons. A similar limitation of neurite growth in neurons with multiple axons was reported previously (Jiang et al., 2005). Multiple axons were also induced by nontagged shootin1 cotransfected with EGFP (43 ± 2.6%; $n = 3$; 67 neurons examined; $P < 0.001$, compared with EGFP), whereas a small population (1.6 ± 1.6%; $n = 3$; 61 neurons examined) of control neurons expressing EGFP formed supernumerary axons, thereby ruling out the possibility that tagging myc to shootin1 influences the effects. These results suggest that the asymmetric accumulation of shootin1 is involved in neuronal polarization.

Repressing shootin1 expression inhibits neuronal polarization

We next suppressed shootin1 expression using a vector-based RNAi system that expresses microRNA (miRNA). To ensure a high level of expression of miRNA before polarization, hippocampal neurons prepared from E18 rat embryo and transfected with the expression vector of a miRNA designated against shootin1 or a control miRNA were plated on polystyrene plates without any coating. After 20 h for the induction of the miRNA expression, the cells were collected and cultured on coverslips coated with polylysine and laminin. The shootin1 miRNA reduced the level of neuronal shootin1 (Fig. 3 F, arrows), in comparison to control neurons (arrowheads) and neurons transfected with the control miRNA. Repression of shootin1 expression by the miRNA led to significant suppression of neuronal polarization at 50 and 70 h in culture, whereas the control miRNA had no such effect (Fig. 3 G). On the other hand, 100% of neurons transfected with the shootin1 miRNA ($n = 25$) became polarized on DIV7. As the 20-h delay in neuronal plating might affect time course of neuronal polarization after plating, we also performed similar experiments using E17 rat embryo. Essentially equivalent data were obtained with E17 rat embryo

(Fig. 3 G). The significant suppression of neuronal polarization by shootin1 RNAi provides evidence that shootin1 is involved in neuronal polarization.

Shootin1 accumulation in growth cones stimulates neurite elongation during the stage 2/3 transition

As described, shootin1 showed fluctuating accumulation in growth cones concurrent with neurite elongation in stage 2 neurons, raising the possibility that shootin1 accumulation in growth cones stimulates neurite elongation. During the stage 2/3 transition, neurites of hippocampal neurons show dynamic elongation and retraction without a remarkable increase in total neurite length (Goslin and Banker, 1989). In addition, the stage 2/3 transition is a critical period of neuronal polarization. Therefore, we examined the effect of shootin1 overexpression and RNAi during this period (24 and 48 h in culture). In contrast to the data of DIV7 (Fig. 3 E) and DIV4, shootin1 overexpression induced a significant increase in total neurite length during this period (Fig. 3 H). Furthermore, repression of its level by RNAi resulted in a significant decrease in it (Fig. 3 I). Along with the time-lapse data, these results suggest that shootin1 accumulation in growth cones stimulates neurite elongation during the transition from stage 2 to 3.

Shootin1 is anterogradely transported to the growth cones with wave-like structures and diffuses back to the soma

We next asked how shootin1 accumulates asymmetrically in hippocampal neurons. As already noted (Fig. 3 A, arrowheads), the series of time-lapse imaging revealed active transport of shootin1 from the cell body to the growth cones in stages 2 and 3 neurons (Fig. 4 A). The shootin1 transport was observed along minor processes and axons. Ruthel and Banker (1998, 1999) reported wave-like anterograde movement of growth cone–like structures along minor processes and axons of cultured hippocampal neurons. The transport rate of these "waves" was ~3 μm/min, similar to that of slow axonal transport component b, which transports actin (Lasek, et al., 1984; Brown, 2003). In addition, waves were enriched in F-actin and their movement was reversibly blocked by the actin-disrupting agent cytochalasin. Therefore, Ruthel and Banker (1998, 1999) suggested that actin and other cytoskeletal components are transported as waves from the cell body to neurite tips via an actin-dependent mechanism. Shootin1 traveled as discrete boluses with growth cone–like structures at a mean rate of 1.0 ± 0.1 μm/min ($n = 12$), which is similar to the speed of wave transport. We occasionally observed transient retrograde transport of GFP-shootin1. However, as in the case of the wave, retrograde transport was rare and short-lived, quickly reverting to anterograde movement. In addition, the boluses of shootin1 were enriched for F-actin (Fig. 4 B) and the transport was arrested by the actin-disrupting agent cytochalasin D within 5 min (Fig. S3 A, available at http://www.jcb.org/cgi/content/full/jcb.200604160/DC1), as reported for the waves. Blebbistatin, an inhibitor of myosin II (Straight et al., 2003), also stopped shootin1 transport (Fig. 4 C). These results suggest that shootin1 is anterogradely transported with the wave-like structure by an actin- and myosin-dependent mechanism.

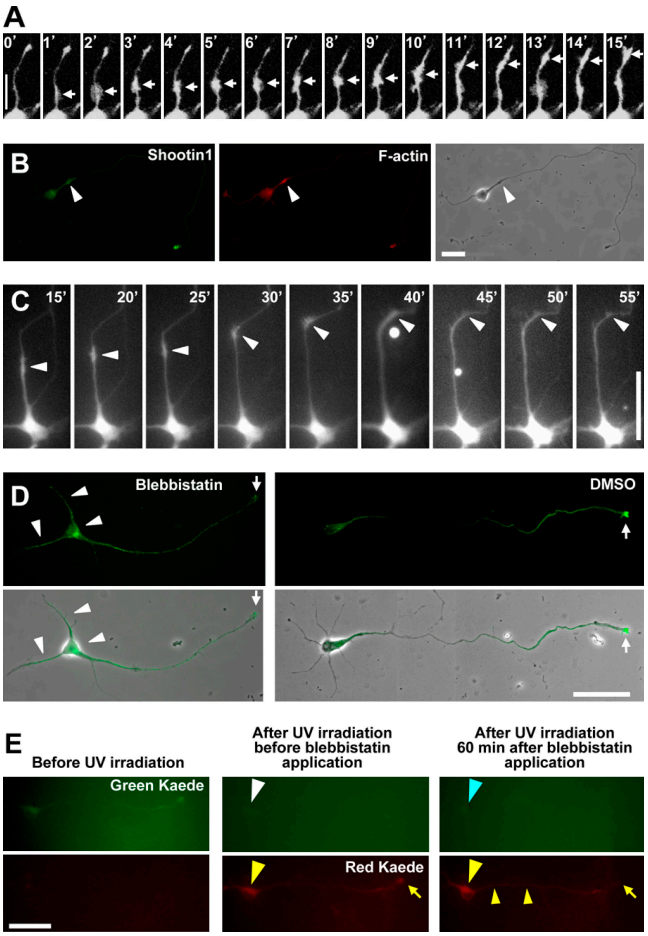

Figure 4. **Shootin1 is anterogradely transported to the growth cones with wave-like structures and diffuses back to the soma.** (A) Distal movements of EGFP-shootin1 within neurite shafts from the cell body to a growth cone. The arrows indicate boluses of EGFP-shootin1. (B) A stage 3 hippocampal neuron double stained with anti-shootin1 antibody and Rhodamine phalloidin. Shootin1- and F-actin–enriched wave is indicated by arrowheads. (C) Serial time-lapse images showing the effect of 50 μM blebbistatin on anterograde transport of EGFP-shootin1. Blebbistatin was applied to the medium for between 35 and 40 min. EGFP-shootin1 in the neurite shaft is indicated by arrowheads. (D) Disturbance of shootin1 transport by blebbistatin inhibits its accumulation in axonal growth cones. Stage 3 hippocampal neurons (cultured for 48 h) were incubated with 50 μM blebbistatin for 1 h and stained with anti-shootin1 antibody. (E) Shootin1 diffuses from the axonal growth cone to the cell body. Kaede-shootin1 expressed in stage 3 hippocampal neurons was converted from green to red using UV light. 1 h after the cessation of shootin1 transport by 50 μM blebbistatin, distributions of red Kaede-shootin1 and newly synthesized green Kaede-shootin1 were examined. Bars: (A and B) 20 μm; (C–E) 50 μm.

Within 2 h of the cessation of the transport by blebbistatin or cytochalasin D, shootin1 accumulation in the axonal growth cones of stage 3 neurons disappeared (Fig. 4 D and Fig. S3 B, arrows) and a relatively high level of shootin1 was observed in the soma, axonal shaft, and minor processes (arrowheads). To examine whether shootin1 returned back from the axonal growth cones to the cell bodies by diffusion or was locally degraded in the growth cones and newly synthesized in the cell body, we used the photoconvertible reporter Kaede (Ando et al., 2002) to distinguish old shootin1 from newly synthesized shootin1.

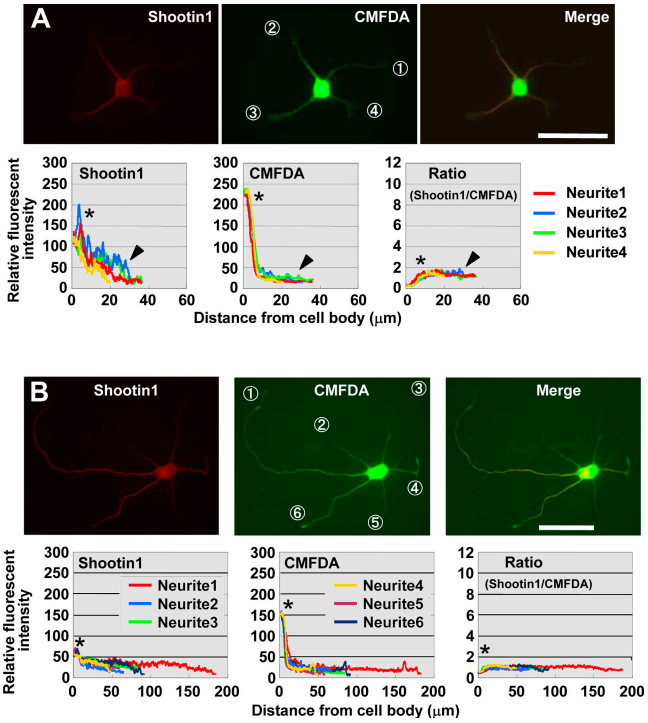

Figure 5. **Inhibition of shootin1 transport prevents its asymmetric accumulation in hippocampal neurons.** (A) Stage 2 hippocampal neurons treated with 50 μM blebbistatin for 1 h were double stained with anti-shootin1 antibody (red) and a volume marker CMFDA (green). Quantitative profiles show the relative fluorescence intensities of shootin1 and CMFDA and the relative concentration of shootin1 (shootin1 immunoreactivity/CMFDA staining) in neurites 1–4. The arrowheads and asterisks denote the minor processes and cell body, respectively. (B) Hippocampal neurons were treated with 50 μM blebbistatin at 14 h in vitro, further cultured for 36 h, and double stained with anti-shootin1 antibody (red) and CMFDA (green). Quantitative profiles show the relative fluorescence intensities of shootin1 and CMFDA and the relative concentration of shootin1 in neurites 1–6. The asterisks denote the cell body. Bars, 50 μm.

Kaede-shootin1 expressed in stage 3 hippocampal neurons was converted from green to red using UV light, and shootin1 transport was blocked by blebbistatin (Fig. 4 E). 1 h after the cessation of shootin1 transport, the accumulation of the red Kaede-shootin1 in the axonal growth cones decreased (Fig. 4 E, yellow arrows), whereas the red fluorescence of Kaede-shootin1 increased in the soma and shaft (yellow arrowheads). On the other hand, we could not detect new synthesis of green Kaede-shootin1 in the soma (Fig. 4 E, blue arrowhead). These data suggest that shootin1 passively diffuses back from the growth cones to the cell bodies.

Inhibition of shootin1 transport prevents its asymmetric accumulation in neurons

We next asked whether the anterograde transport of shootin1 is involved in its asymmetric accumulation in hippocampal neurons. As shown in Fig. 5 A and Fig. S3 C, cessation of shootin1 transport in stage 2 neurons by blebbistatin or cytochalasin D prevented accumulation of shootin1 in multiple growth cones. Stage 2 neurons were cultured for 36 h in the presence of blebbistatin or cytochalasin D. As described, in control neurons, shootin1 accumulates asymmetrically in growth cones of nascent axons during this period. On the other hand, shootin1 did not accumulate in single neurites in the presence of these drugs (Fig. 5 B and Fig. S3 D). Cessation of shootin1 transport in already polarized stage 3 neurons also prevented accumulation of shootin1 in axonal growth cones, as described (Fig. 4 D and Fig. S3 B). These data indicate that the actin- and myosin-dependent anterograde transport of shootin1 is necessary for its asymmetric accumulation in single growth cones.

Shootin1 regulates the localization of PI 3-kinase activity in hippocampal neurons

Recent studies indicate that PI 3-kinase is located at a critical upstream position in signaling pathways for neuronal polarization (Arimura and Kaibuchi, 2005; Wiggin et al., 2005). We finally examined whether shootin1 interacts with the PI 3-kinase pathway. The physiological association of shootin1 and PI 3-kinase was examined by coimmunoprecipitation assay. When shootin1 was immunoprecipitated from P5 rat brain lysates, coimmunoprecipitation of the p85 subunit of PI 3-kinase was detected (Fig. 6 A). Shootin1 was also reciprocally coimmunoprecipitated with p85, indicating that it associates with p85 in vivo. PI 3-kinase activity, indirectly visualized by the phosphorylation of Akt at Ser473 (P-Akt), was enriched in the axonal growth cones of stage 3 neurons (Fig. 6 B, arrows) as reported (Shi et al., 2003) and preferentially colocalized there with shootin1 (Fig. 6 B, insets). We exogenously coexpressed shootin1 and p85 in HEK293T cells but could not detect coimmunoprecipitation between shootin1 and p85 (not depicted). Thus, shootin1 may interact with PI 3-kinase through unidentified neuronal proteins. As shown recently (Yoshimura et al., 2006), overexpression of constitutively active PI 3-kinase (Myr-PI 3-K p110) induced formation of multiple axons (Fig. 6 H and Fig. S4 B, available at http://www.jcb.org/cgi/content/full/jcb.200604160/DC1), as in the case of shootin1 overexpression. Jiang et al. (2005) also reported that overexpression of constitutively active Akt (Myr-Akt), a downstream kinase of PI 3-K, induced formation of multiple axons. On the other hand, inhibition of PI 3-kinase activity by 20 μM LY294002, a specific inhibitor of PI 3-kinase, delayed neuronal polarization (Fig. 6 C), as reported previously (Menager et al., 2004) and as in the case of shootin1 RNAi. These results suggest that shootin1 interacts with PI 3-kinase and is involved in a similar pathway mediating neuronal polarity.

Next, we examined whether shootin1 functions upstream of PI 3-kinase or vice versa. Shootin1 RNAi decreased its level in axonal growth cones, which in turn inhibited accumulation of PI 3-kinase activity there (Fig. 6 D, arrows), suggesting that shootin1 in axonal growth cones is required for accumulation of PI 3-kinase activity there. Conversely, myc-shootin1 overexpression induced its ectopic accumulation in the growth cones of minor processes, which in turn resulted in ectopic accumulation there of P-Akt (Fig. 6 E, arrowheads), thereby suggesting that accumulation of shootin1 can recruit PI 3-kinase activity. On the other hand, inhibition of PI 3-kinase activity by LY294002 did not affect the accumulation of shootin1 in axonal growth cones (Fig. 6 F, arrows). Shootin1 overexpression or RNAi did not change the activity of PI 3-kinase in hippocampal

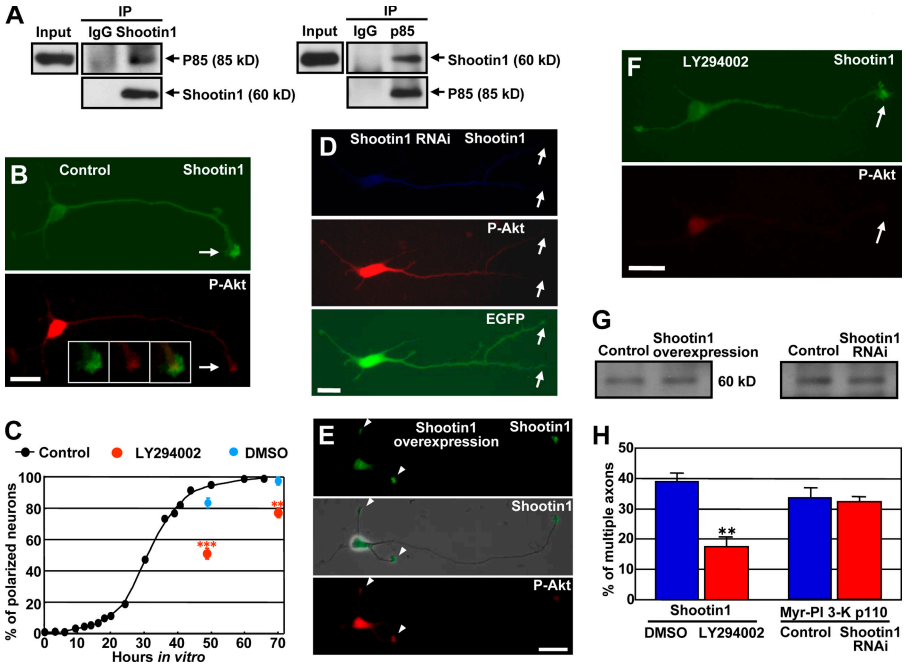

Figure 6. **Shootin1 regulates the localization of PI 3-kinase activity in hippocampal neurons.** (A) Brain lysates from P5 rat brain were incubated with anti-shootin1 antibody, anti-p85 antibody, or control IgG. The immunoprecipitates were analyzed by immunoblotting with anti-shootin1 and anti-p85 antibodies as indicated. (B) Stage 3 hippocampal neurons were incubated with DMSO as control for 10 h and double stained with anti-shootin1 antibody and anti–P-Akt (Ser473) antibody. Arrows indicate an axonal growth cone. Note that PI 3-kinase activity was preferentially colocalized with shootin1 in the axonal growth cone (insets). (C) Neurons were cultured in the normal medium or in the presence of 20 μM LY294002 or DMSO. Data present percentages of neurons bearing axons (stage 3 neurons) as means ± SE (**, $P < 0.005$; ***, $P < 0.002$; $n = 3$; a total of 699 neurons were examined). (D) Stage 3 neurons transfected with the miRNA against shootin1 were double stained with anti-shootin1 antibody (blue) and anti–P-Akt antibody (red). The vector for the miRNA expressions is designed to coexpress EGFP (green). Arrows indicate a shootin1-immunonegative axonal growth cone without remarkable accumulation of P-Akt. (E) Shootin1 overexpressed in stage 3 neurons accumulated ectopically in minor processes together with P-Akt (arrowheads). (F) Stage 3 hippocampal neurons were incubated with 20 μM LY294002 for 10 h and double stained with anti-shootin1 antibody and anti–P-Akt antibody. Arrows indicate a P-Akt–immunonegative axonal growth cone with remarkable shootin1 accumulation. (G) Primary cultured hippocampal neurons were transfected by pCAGGS-myc-shootin1 or pCAGGS-myc-GST (control; left) or were transfected with the miRNA against shootin1 or a control miRNA (right) using Nucleofector. The efficiency of transfection was >80%. After 36 h in culture, cell lysates were collected and immunoblotted by anti–P-Akt antibody to monitor PI 3-kinase activity. (H) Hippocampal neurons overexpressing myc-shootin 1 were cultured for 7 d in the presence of 20 μM LY294002 or DMSO ($n = 3$; 198 neurons examined). Neurons transfected with pCAGGS–Myr–PI 3-kinase p110 plus the miRNA against shootin1 or pCAGGS–Myr–PI 3-kinase p110 plus a control-miRNA were also cultured for 7 d ($n = 3$; 225 neurons examined). Data present percentages of neurons with multiple axons as means ± SE. **, $P < 0.001$. Bars, 20 μm.

neurons (Fig. 6 G), ruling out the possibility that the expression level of shootin1 changes the total activity of PI 3-kinase in neurons. These results suggest that shootin1 regulates subcellular localization of PI 3-kinase activity in hippocampal neurons.

We further examined the functions of shootin1 and PI 3-kinase within the cell polarity pathways. Inhibition of PI 3-kinase activity by LY294002 led to a reduction in the percentage of neurons with multiple axons induced by shootin1 overexpression (Fig. 6 H and Fig. S4 A). On the other hand, multiple axon formation by overexpression of constitutively active PI 3-kinase was not inhibited by shootin1 RNAi (Figs. 6 H and Fig. S4 B). Collectively, these results provide evidence that shootin1 functions upstream of PI 3-kinase and is required for spatially localized PI 3-kinase activity, which is essential for neuronal polarization (Shi et al., 2003).

Discussion

We have identified a novel brain-specific protein, shootin1, using highly sensitive 2DE-based proteomics. The spatiotemporal localization of shootin1 in hippocampal neurons changed dynamically during polarization: it became up-regulated, began fluctuating accumulation among multiple neurites, and eventually accumulated asymmetrically in a single neurite, which led to axon induction for polarization. Disturbing the asymmetric organization of shootin1 by excess shootin1 induced formation of multiple axons, whereas repressing shootin1 expression inhibited polarization. These results suggest that shootin1 plays a critical role in neuronal polarization.

Shootin1 in generation of an asymmetric signal for neuronal polarization

How does the symmetric localization of shootin1 shift to asymmetric localization before polarization? Does shootin1 spontaneously organize its own polarized distribution without asymmetric cues? Two types of regulation have been postulated for a mechanism that accounts for spontaneous neuronal polarization (Craig and Banker, 1994; Andersen and Bi, 2000). One is a positive feedback loop acting locally in neurites, where a stochastic increase in signals is enhanced until their level exceeds a threshold to induce an axon. If accumulation of a particular molecule in growth cones stimulates neurite elongation and if its accumulation increases in proportion to neurite length, such a molecule can constitute the positive feedback loop to enhance its own signal for axon formation (Goslin and Banker, 1990; Craig and Banker, 1994). Our data suggest that shootin1 accumulation in growth cones stimulates neurite elongation during the stage 2/3 transition. In addition, shootin1 may accumulate in growth cones in a neurite length–dependent manner, as it is actively transported from the cell body to growth cones and its retrograde diffusion to the cell body should vary inversely with neurite length (Goslin and Banker, 1989). Consistent with this notion, inhibiting the anterograde transport of shootin1 disturbed its asymmetric accumulation in neurons. Thus, shootin1

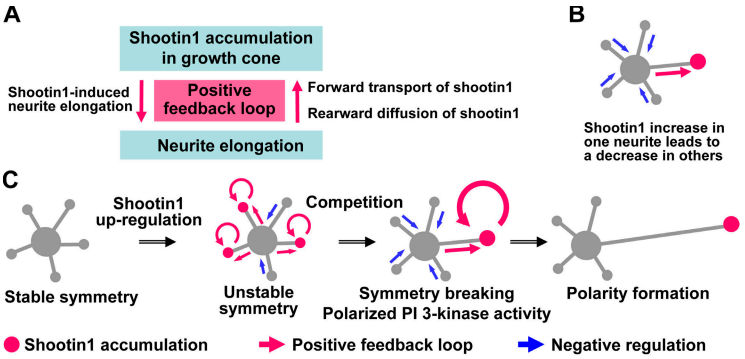

Figure 7. **A model for the involvement of shootin1 in generation of an asymmetric signal for neuronal polarization.** (A) A positive feedback loop between shootin1 accumulation in growth cone and shootin1-induced neurite elongation. (B) Competition among neurites for a limited amount of shootin1. (C) Shootin1 up-regulation triggers local positive feedback loops (red arrows) and negative regulations (blue arrows). Eventually, shootin1 will be asymmetrically accumulated in a single neurite and recruit PI 3-kinase activity there, thereby leading to neuronal polarization.

is a good candidate molecule for the requisite positive feedback loop for axon induction (Fig. 7 A).

The second component is negative regulation to prevent the formation of surplus axons (Craig and Banker, 1994; Andersen and Bi, 2000). Because the concentration of shootin1 in the cell body is very low and limited throughout stages 2 and 3, the aforementioned positive feedback loop may elicit competition among neurites for a limited amount of shootin1: an increase in shootin1 in one growth cone may lead to a decrease in sibling growth cones (Fig. 7 B). Indeed, sustained accumulation of shootin1 in one growth cone reduced levels in its sibling neurites. Furthermore, excess levels of shootin1 prevented its redistribution and induced the formation of surplus axons. Thus, the negative regulation to prevent formation of surplus axons may be achieved by competition among neurites for a limited amount of shootin1.

Fig. 7 C shows our current model in which shootin1 generates an asymmetric signal for neuronal polarization. In this model, shootin1 up-regulation triggers the aforementioned positive and negative regulation, which shifts the symmetry of neurons from a stable to an unstable state. Eventually, shootin1 accumulates asymmetrically in a single neurite, through amplification of its stochastic signals and competitive accumulation among neurites, thereby leading to neuronal polarization.

Shootin1 and previously described mechanisms for neuronal polarization

Recent papers indicate that PI 3-kinase is located at an upstream position in signaling pathways for neuronal polarization involving many molecules, such as phosphatidylinositol (3,4,5) triphosphate, the mPar3–mPar6–aPKC complex, Cdc42, Rap1B, STEF/Tiam1, Rac, Akt, adenomatous polyposis coli, glycogen synthase kinase-3β, and collapsin response mediator protein-2 (Shi et al., 2003; Arimura and Kaibuchi, 2005; Wiggin et al., 2005). We found that shootin1 interacts with PI 3-kinase and is required for spatially localized PI 3-kinase activity in hippocampal neurons. Furthermore, a series of overexpression and loss of function studies suggested that shootin1 functions upstream of PI 3-kinase in regulating neuronal polarity. Thus, shootin1 may be involved in the organization of polarized PI 3-kinase activity (Fig. 7 C), which is essential for neuronal polarization (Shi et al., 2003).

Recently, Jacobson et al. (2006) showed time-lapse imaging of the motor domain of kinesin-1 in cultured hippocampal neurons. As in the case of shootin1, the kinesin-1 motor domain transiently accumulated in different minor processes of stage 2 neurons and selectively and continuously accumulated in the nascent axon during the stage 2/3 transition, thereby indicating that it serves as a very early marker for the symmetry breaking event. The present data showed that shootin1 accumulation in growth cones was induced by the actin- and myosin-dependent wave-like transport and stimulated neurite elongation. On the other hand, the accumulation of the kinesin-1 motor domain may be dependent on microtubule and was not related to neurite elongation. It is intriguing to analyze how these molecules interact during polarization.

In addition to internal signals for polarization, additional external cues are likely to adjust the orientation of an axon and dendrites in situ. Although the identities of such cues in the brain are not yet clear, Esch et al. (1999) reported that the spatially asymmetric extracellular signals of laminin and neuron-glia cell adhesion molecule can specify which neurite will become an axon under experimental conditions. The present study does not rule out the possibility that shootin1 is modified by other molecules. By regulating the activity of shootin1, additional molecules might further adjust the orientation of an axon and dendrites in situ.

In conclusion, we have identified shootin1, a novel protein involved in neuronal polarization. Based on the present findings, we proposed a model in which shootin1 expression triggers the positive and negative regulation required for neuronal symmetry breaking. Although we cannot rule out the involvement of other potential mechanisms, our data provide an insight into how internal asymmetric signals are generated during neuronal polarization.

Materials and methods

Cultures and metabolic labeling

Hippocampal neurons prepared from E18 rat embryos were cultured as described previously (Inagaki et al., 2001). For hippocampal explant culture, the hippocampi dissected from E18 rat embryos were cut into blocks (~1 mm), carefully washed to remove dissociated cells, and cultured on polylysine- and laminin-coated plastic dishes. The explants started to extend radial axons on the dishes within 12 h. On DIV14, the radial axons formed complicated networks around the explants. The axonal networks were usually devoid of cell bodies, dendrites, and nonneuronal cells (Fig. 1 B), although we occasionally observed migration of neurons from blocks onto axonal networks. Such cells were rigorously removed under a microscope using pipette tips. Explants containing somatodendritic parts were separated from radial axons by applying streams of medium to the explants with a pipette, and the explants were then collected in microcentrifuge tubes.

Removal of the explants and dissociated cells from axon networks was verified by microscopy.

For quantitative 2DE, stages 2 and 3 neurons were metabolically labeled with the culture medium containing 13% of the normal levels of methionine and cysteine plus Pro-mix L-[^{35}S] in vitro cell labeling mix (containing ~70% L-[^{35}S]methionine and ~30% L-[^{35}S]cysteine; GE Healthcare) for 4 h. Hippocampal explants were labeled with the same medium for 24 h.

Highly sensitive gel 2DE and protein identification by mass spectrometry

2DE was performed as reported previously (Oguri et al., 2002), using a 93- × 103-cm large-gel system (Inagaki and Katsuta, 2004). For differential 2DE, neurons or explants were metabolically labeled and protein spots separated by 2DE gels were visualized by autoradiography. For protein identification, unlabeled protein samples from 2-wk-old rat brains were separated by the 2DE gel and visualized by silver staining. The protein spots corresponding to the radio-labeled ones were then excised from gels and in-gel digested as described previously (Nomura et al., 2004). Matrix-assisted laser desorption/ionization mass spectrometry was performed using a Voyager Elite equipped with delayed extraction (Applied Biosystems). Database searches were conducted using the Mascot program (Matrix Science) and National Center for Biotechnology Information databases.

Cloning of shootin1

cDNA encoding KIAA1598 was provided by T. Nagase and O. Ohara (Kazusa DNA Research Institute, Chiba, Japan). Full-length cDNA of human *shootin1* was obtained by PCR of KIAA1598 with the primers 5′-GCGGATCCATGAACAGCTCGGACGAAGAGAAGCAGCTGCAGCTCATTACCAGTCTGAAG and 5′-GCGGATCCCTACTGGGAGGCCAGTATTC. cDNA encoding rat *shootin1* was amplified by PCR from a rat brain cDNA library (CLONTECH Laboratories, Inc.) with the primers 5′-CCGCTCGAGATGAACAGCTCGGACGAGGAGAAG and 5′-CCGCTCGAGTTACTGGGAGGCCAGGATTCCCTTCAG. The cDNAs were then subcloned into pCMV (Stratagene), pCAGGS with a β-actin promoter (provided by J. Miyazaki, Osaka University, Osaka, Japan; Niwa et al., 1991), pEGFP (CLONTECH Laboratories, Inc.), pGEX (GE Healthcare), and pKaede-MC1 (MBL International Corporation) vectors.

Protein and antibody preparation

Recombinant shootin1 was expressed in *Escherichia coli* as a GST fusion protein and purified on a glutathione–Sepharose column (GE Healthcare), after which GST was removed from shootin1 by PreScission protease (GE Healthcare). Rabbit polyclonal anti-shootin1 antibody was raised against the recombinant shootin1 and affinity purified before use.

Immunocytochemistry, immunoblot, and immunoprecipitation

Immunocytochemistry, CMFDA staining, Rhodamine phalloidin staining, and immunoblot were performed as described previously (Inagaki et al., 2001). For immunoprecipitation, P4 or P5 rat brains were extracted by addition of lysis buffer (50 mM Tris-HCl, pH 8.0, 1 mM EDTA, 150 mM NaCl, 1% Triton X-100, 0.1% SDS, 0.1% sodium deoxycholate, 2 mM phenylmethylsulfonyl fluoride, 5 μg/ml leupeptin, 10 mM NaF, 1 mM Na_3VO_4, and 10 mM β-glycerophosphate) and centrifuged at 100,000 *g* for 30 min at 4°C. The supernatants were incubated with antibodies overnight at 4°C, and immunocomplexes were then precipitated with protein G–Sepharose 4B (GE Healthcare). After washing out beads with RIPA buffer, immunocomplexes were analyzed by immunoblot.

Microscopy

Fluorescent and phase-contrast images of neurons were acquired at room temperature using a fluorescent microscope (Axioplan 2; Carl Zeiss MicroImaging, Inc.) equipped with a Plan-NEOFLUAR 40×, 0.75 NA, or 20×, 0.50 NA, objective, a charge-coupled device camera (AxioCam MRm; Carl Zeiss MicroImaging, Inc.), and imaging software (AxioVision 3; Carl Zeiss MicroImaging, Inc.). Time-lapse microscopy was performed at 37°C using a fluorescent microscope (Axiovert S100; Carl Zeiss MicroImaging, Inc.) equipped with a Plan-NEOFLUAR 40×, 1.3 NA oil iris objective, CSNAP, and Deltavision 2 (Applied Precision) software or Axiovert 200M (Carl Zeiss MicroImaging, Inc.) equipped with a Plan-NEOFLUAR 40×, 0.75 NA objective, LSM 510 scan module (Carl Zeiss MicroImaging, Inc.), and LSM 510 META software (Carl Zeiss MicroImaging, Inc.). The acquired images were analyzed with Multi Gauge (Fujifilm) or LSM510 META software.

Transfection and RNAi

Neurons or HEK293T cells were transfected with cDNA or RNA by the calcium phosphate method (Inagaki et al., 2001), Nucleofector (Amaxa), or Lipofectamine 2000 (Invitrogen) before or after plating. For vector-based RNAi analysis, we used BLOCK-iT Pol II miR RNAi expression vector kit (Invitrogen). The targeting mRNA sequence TGAAGCTGTTAAGAAACTGGA corresponds to nucleotides 138–158 in the coding region of rat shootin1, whereas the control vector pcDNA 6.2-GW/EmGFP-miR-neg encodes an mRNA not to target any known vertebrate gene.

Materials

Antibodies against myc, tau-1, synaptophysin, MAP-2, α-tubulin, the p85 subunit of PI 3-kinase, and monoclonal (587F11) phospho-Akt (Ser473) were obtained from MBL International Corporation, Boehringer, Progen, Sigma-Aldrich, Sigma-Aldrich, Upstate Biotechnology, and Cell Signaling Technology, respectively. CMFDA, Rhodamine phalloidin, blebbistatin, cytochalasin D, and LY294002 were obtained from Invitrogen, Invitrogen, BIOMOL Research Laboratories, Inc., Calbiochem, and Calbiochem, respectively. cDNA encoding Myr-PI 3-K p110 was obtained from Upstate Biotechnology. mRFP was provided by R. Tsien (University of California, San Diego, La Jolla, CA).

Online supplemental material

Fig. S1 shows serial time-lapse images of EGFP-shootin1 accumulation in neurites 1 and 2 of Fig. 2 (D–G). Fig. S2 shows DIV7 hippocampal neurons overexpressing myc-shootin1, which are immunostained by anti-synaptophysin or anti–MAP-2 antibody. Fig. S3 shows the effects of cytochalasin D on shootin1 distribution in hippocampal neurons. Fig. S4 shows that inhibition of PI 3-kinase activity suppresses formation of shootin1-induced multiple axons, but repression of shootin1 expression by RNAi does not inhibit formation of PI 3-kinase–induced multiple axons. Video 1 is a time-lapse video of a stage 2 hippocampal neuron expressing EGFP-shootin1 as described in Fig. 2 A. Video 2 is a time-lapse video of a hippocampal neuron expressing EGFP-shootin1 taken from stages 2 to 3 as described in Fig. 2 (D–G). Video 3 is a time-lapse video of a hippocampal neuron overexpressing EGFP-shootin1 as described in Fig. 3 A. Online supplemental material is available at http://www.jcb.org/cgi/content/full/jcb.200604160/DC1.

We thank Dr. Goro Eguchi and the advisors of Recognition and Formation, Precursory Research for Embryonic Science and Technology, for suggestions; Drs. Hiroshi Itoh, Sadao Shiosaka, Kazunori Imaizumi, and Shin Ishii for discussion; Drs. Mu-ming Poo and Ian Smith for reviewing the manuscript; Drs. Takahiro Nagase and Osamu Ohara for providing the cDNA encoding KIAA1598; and Ms. Kumiko Motegi for secretarial assistance. We also thank Drs. Jun-ichi Miyazaki and Roger Y. Tsien for providing pCAGGS and mRFP vectors, respectively.

This research was supported in part by Precursory Research for Embryonic Science and Technology at Japanese Science and Technology Corporation; the Ministry of Education, Sports, Culture, Science and Technology (18300107); and the Japan Society for the Promotion of Science KAKENHI (18016020 and 18022028), the Suntory Institute for Bioorganic Research, and the Osaka Medical Research Foundation for Incurable Diseases.

Submitted: 26 April 2006
Accepted: 18 September 2006

References

Andersen, S.S., and G.Q. Bi. 2000. Axon formation: a molecular model for the generation of neuronal polarity. *Bioessays.* 22:172–179.

Ando, R., H. Hama, M. Yamamoto-Hino, H. Mizuno, and A. Miyawaki. 2002. An optical marker based on the UV-induced green-to-red photoconversion of a fluorescent protein. *Proc. Natl. Acad. Sci. USA.* 99:12651–12656.

Arimura, N., and K. Kaibuchi. 2005. Key regulators in neuronal polarity. *Neuron.* 48:881–884.

Banker, G. 2003. Pars, PI 3-kinase, and the establishment of neuronal polarity. *Cell.* 112:4–5.

Bradke, F., and C.G. Dotti. 1999. The role of local actin instability in axon formation. *Science.* 283:1931–1934.

Brown, A. 2003. Axonal transport of membranous and nonmembranous cargoes: a unified perspective. *J. Cell Biol.* 160:817–821.

Craig, A.M., and G. Banker. 1994. Neuronal polarity. *Annu. Rev. Neurosci.* 17:267–310.

Da Silva, J.S., and C.G. Dotti. 2002. Breaking the neuronal sphere: regulation of the actin cytoskeleton in neuritogenesis. *Nat. Rev. Neurosci.* 3:694–704.

Dotti, C.G., and G.A. Banker. 1987. Experimentally induced alteration in the polarity of developing neurons. *Nature.* 330:254–256.

Dotti, C.G., C.A. Sullivan, and G.A. Banker. 1988. The establishment of polarity by hippocampal neurons in culture. *J. Neurosci.* 8:1454–1468.

Esch, T., V. Lemmon, and G. Banker. 1999. Local presentation of substrate molecules directs axon specification by cultured hippocampal neurons. *J. Neurosci.* 19:6417–6426.

Goslin, K., and G. Banker. 1989. Experimental observations on the development of polarity by hippocampal neurons in culture. *J. Cell Biol.* 108:1507–1516.

Goslin, K., and G. Banker. 1990. Rapid changes in the distribution of GAP-43 correlate with the expression of neuronal polarity during normal development and under experimental conditions. *J. Cell Biol.* 110:1319–1331.

Horton, A.C., and M.D. Ehlers. 2003. Neuronal polarity and trafficking. *Neuron.* 40:277–295.

Inagaki, N., and K. Katsuta. 2004. Large gel two-dimensional electrophoresis: improving recovery of cellular proteome. *Current Proteomics.* 1:35–39.

Inagaki, N., K. Chihara, N. Arimura, C. Menager, Y. Kawano, N. Matsuo, T. Nishimura, M. Amano, and K. Kaibuchi. 2001. CRMP-2 induces axons in cultured hippocampal neurons. *Nat. Neurosci.* 4:781–782.

Jacobson, C., B. Schnapp, and G.A. Banker. 2006. A change in the selective translocation of the Kinesin-1 motor domain marks the initial specification of the axon. *Neuron.* 49:797–804.

Jiang, H., W. Guo, X. Liang, and Y. Rao. 2005. Both the establishment and the maintenance of neuronal polarity require active mechanisms: critical roles of GSK-3β and its upstream regulators. *Cell.* 120:123–135.

Lasek, R.J., J.A. Garner, and S.T. Brady. 1984. Axonal transport of the cytoplasmic matrix. *J. Cell Biol.* 99:212s–221s.

Menager, C., N. Arimura, Y. Fukata, and K. Kaibuchi. 2004. PIP3 is involved in neuronal polarization and axon formation. *J. Neurochem.* 89:109–118.

Nishimura, T., T. Yamaguchi, K. Kato, M. Yoshizawa, Y. Nabeshima, S. Ohno, M. Hoshino, and K. Kaibuchi. 2005. PAR-6-PAR-3 mediates Cdc42-induced Rac activation through the Rac GEFs STEF/Tiam1. *Nat. Cell Biol.* 7:270–277.

Niwa, H., K. Yamamura, and J. Miyazaki. 1991. Efficient selection for high-expression transfectants with a novel eukaryotic vector. *Gene.* 108:193–199.

Nomura, E., K. Katsuta, T. Ueda, M. Toriyama, T. Mori, and N. Inagaki. 2004. Acid-labile surfactant improves in-sodium dodecyl sulfate polyacrylamide gel protein digestion for matrix-assisted laser desorption/ionization mass spectrometric peptide mapping. *J. Mass Spectrom.* 39:202–207.

Oguri, T., I. Takahata, K. Katsuta, E. Nomura, M. Hidaka, and N. Inagaki. 2002. Proteome analysis of rat hippocampal neurons by multiple large gel two-dimensional electrophoresis. *Proteomics.* 2:666–672.

Rolls, M.M., and C.Q. Doe. 2004. Baz, Par-6 and aPKC are not required for axon or dendrite specification in *Drosophila*. *Nat. Neurosci.* 7:1293–1295.

Ruthel, G., and G. Banker. 1998. Actin-dependent anterograde movement of growth-cone-like structures along growing hippocampal axons: a novel form of axonal transport? *Cell Motil. Cytoskeleton.* 40:160–173.

Ruthel, G., and G. Banker. 1999. Role of moving growth cone-like "wave" structures in the outgrowth of cultured hippocampal axons and dendrites. *J. Neurobiol.* 39:97–106.

Schwamborn, J.C., and A.W. Puschel. 2004. The sequential activity of the GTPases Rap1B and Cdc42 determines neuronal polarity. *Nat. Neurosci.* 7:923–929.

Shi, S.H., L.Y. Jan, and Y.N. Jan. 2003. Hippocampal neuronal polarity specified by spatially localized mPar3/mPar6 and PI 3-kinase activity. *Cell.* 112:63–75.

Shi, S.H., T. Cheng, L.Y. Jan, and Y.N. Jan. 2004. APC and GSK-3beta are involved in mPar3 targeting to the nascent axon and establishment of neuronal polarity. *Curr. Biol.* 14:2025–2032.

Straight, A.F., A. Cheung, J. Limouze, I. Chen, N.J. Westwood, J.R. Sellers, and T.J. Mitchison. 2003. Dissecting temporal and spatial control of cytokinesis with a myosin II inhibitor. *Science.* 299:1743–1747.

Wiggin, G.R., J.P. Fawcett, and T. Pawson. 2005. Polarity proteins in axon specification and synaptogenesis. *Dev. Cell.* 8:803–816.

Winckler, B., and I. Mellman. 1999. Neuronal polarity: controlling the sorting and diffusion of membrane components. *Neuron.* 23:637–640.

Yoshimura, T., Y. Kawano, N. Arimura, S. Kawabata, A. Kikuchi, and K. Kaibuchi. 2005. GSK-3β regulates phosphorylation of CRMP-2 and neuronal polarity. *Cell.* 120:137–149.

Yoshimura, T., N. Arimura, Y. Kawano, S. Kawabata, S. Wang, and K. Kaibuchi. 2006. Ras regulates neuronal polarity via the PI3-kinase/Akt/GSK-3β/CRMP-2 pathway. *Biochem. Biophys. Res. Commun.* 340:62–68.